

# Velocity Field Estimation Using GPS Precise Point Positioning: The South American Plate Case

J. A. S. Perez; J. F. G. Monico and J. C. Chaves

Faculty of Science and Technology - UNESP, Department of Cartography, Rua Roberto Simonsen, 305, CEP: 19060-900 Presidente Prudente, São Paulo, Brazil  
e-mail: galera@prudente.unesp.br, Tel: 55 18 229-5325; Fax: 223-2227

Received: 4 October 2002 / Accepted: 6 December 2003

**Abstract.** GPS is essential in applications that require high (sub centimeter) positioning precision, such as in the velocity field estimation of tectonic plates. Normally, GPS relative positioning is used for this kind of application. However, GPS Precise Point Positioning (PPP) is a very simple and efficient method, which, as shown in this paper, can also be applied. This paper outlines the use of PPP for processing GPS data. Station coordinates and velocity vectors are inferred, and an estimation of the South American Plate rotation parameters ( $\Omega_x$ ,  $\Omega_y$  and  $\Omega_z$ ) is given. The PPP repeatability of station coordinates is better than 9mm, and comparisons of the final solution with other sources, such as ITRF, NNR-NUVEL 1A and APKIM 2000 generally show good agreement. The formal precision of the station velocity is in the order of 0.6 mm/year, for horizontal and vertical components, which appears to be an optimistic value, and the quality of the estimated rotation parameters is better than those from other sources.

**Key words:** GPS; Geodynamics; Tectonic Plates; Precise Point Positioning

## 1 Introduction

Geodetic coordinates of points on the surface of tectonic plates change with time due to plate motion, and thus become dependent of the epoch in which the coordinates were obtained. If these elements (direction and magnitude) are known, it is possible to determine the change of the point coordinates as a function of time.

Since the 1980's, GPS has provided an ideal technique for supporting this type of research, either for regional or

global applications, because of the low equipment costs and high precision (Parkinson, 1996; Sá, 1999). The contribution of GPS to geodynamics was further developed with the implementation of the IGS (International GPS Service) network, in 1994. Nowadays, there are more than 400 stations composing the IGS network, providing very important coordinate and monitoring information.

RBMC (Brazilian Continuous GPS Network) is an active geodetic network, established in Brazil in 1997 (Fortes, 1997). At that time, 9 stations were operational. Nowadays, there are a total of 15 stations. RBMC is a network of fundamental importance for the continuous monitoring of plate movements within the Brazilian territory.

The main objective of this paper is to estimate and infer coordinates and velocity vectors of a set of stations, and to provide South America (SOAM) plate rotation parameters ( $\Omega_x$ ,  $\Omega_y$  and  $\Omega_z$ ) using GPS PPP. The results are compared with those from the ITRF (International Terrestrial Reference Frame) 2000 solution and the geophysical plate models, NNR-NUVEL 1A (No Net Rotation – Northwestern University VELOCITY model 1A) and APKIM 2000 (Actual Plate Kinematic Model – version 2000).

Nowadays, the monitoring of station coordinates located on the Earth's surface is of enormous interest. Determination of velocity fields provides a means of analysing inter- and intra-plate geodynamic interactions and other types of crustal disturbances.

In South America, velocity field determination is of extreme importance, due to the recent decision to adopt the SIRGAS (Geocentric Reference System for Americas) geocentric reference frame, in which a velocity field is required. However, the two SIRGAS campaigns provided station coordinates only, without a velocity field (see <http://www.ibge.gov.br/home/>

geografia/geodesico/sirgas - access date: October 20, 2003).

In this paper an introduction to plate tectonics is initially given, followed by the basic theory behind the GPS observables and PPP. In the methodology section the software, data set and processing strategy are described. The results are then presented and analysed, followed by comments and conclusions of the research.

## 2 A Brief Introduction to Plate Tectonics

The plate tectonics theory provides an explanation of the movement and deformation of the lithosphere, which comprises of the crust and the uppermost part of the upper mantle. The lithosphere is divided into distinct tectonic plates, and these plates move relative to one another along their boundaries. New lithosphere is created on constructive plate boundaries along ocean ridges, whilst at destructive boundaries the lithosphere returns to the mantle by subduction. For further reading on plate tectonics theory and modeling refer to, Condie (1989), Press & Siever (1986), Turcotte & Schubert (2001) and Drewes (1993).

The study of plate tectonics involves several disciplines such as structural geology, geophysics, petrology and geochemistry, stratigraphy, sedimentology, and paleontology. Research into seismology, seafloor spreading and thermal convection in the mantle provide the geophysical information for the derivation of plate tectonic kinematic models.

In models such as the NNR-NUVEL 1A the global crustal deformations are, in a first approximation, described by the motions of rigid plates (i.e., spherical segments of the globe). The IERS (International Earth Rotation Service) has adopted the kinematic plate model NNR-NUVEL 1A to derive velocity vectors for stations without estimated velocities (McCarthy, 1996).

NNR-NUVEL 1A model assumes No Net Rotation (NNR), which is based on the premise that resulting torques do not exist in the lithosphere. However, GPS provides a better approximation for the estimation of the rotation parameters ( $\Omega_X$ ,  $\Omega_Y$  and  $\Omega_Z$ ) for any plate, particularly the South American Plate (Drewes, 1996; Costa, 1999; Perez, 2002), since it is independent of this premise.

The APKIM 2000, developed at DGFI (Deutsches Geodatisches Forschungsinstitut), is generated from GPS, VLBI (Very Long Baseline Interferometry) and SLR (Satellite Laser Ranging) technologies.

## 3 GPS Observables and PPP

The basic GPS observables used for estimating position, velocity and time are:

Pseudo range; and

Carrier phase or difference of carrier phase.

Precise Point Positioning (PPP), together with relative positioning, provides a significant contribution to geodynamic applications. One of the advantages of PPP is that positions are independently derived. Whereas in relative positioning, an error in the base station coordinates would translate into the other stations. In PPP, dual-frequency data is essential. Therefore, there are two observation equations, for both pseudo range and carrier phase. Considering a station  $A$  and satellite  $j$ , the linearized observations can be written as (Monico and Perez, 2001; Monico, 2000a):

$$E(\Delta PD_{L_1}) = a_A^j \Delta X_A + b_A^j \Delta Y_A + c_A^j \Delta Z_A + c(dt_A - dt^j) + T_A^j + I_A^j \quad (1)$$

$$E(\Delta PD_{L_2}) = a_A^j \Delta X_A + b_A^j \Delta Y_A + c_A^j \Delta Z_A + c(dt_A - dt^j) + T_A^j + \bar{I}_A^j$$

$$E(\lambda_1 \Delta \phi_{A1}^j) = a_A^j \Delta X_A + b_A^j \Delta Y_A + c_A^j \Delta Z_A + c(dt_A - dt^j) + T_A^j - I_A^j + \lambda_1 [\phi^j(t_0)_1 - \phi_A(t_0)_1 + N_{A1}^j] \quad (2)$$

$$E(\lambda_2 \Delta \phi_{A2}^j) = a_A^j \Delta X_A + b_A^j \Delta Y_A + c_A^j \Delta Z_A + c(dt_A - dt^j) + T_A^j - \bar{I}_A^j + \lambda_2 [\phi^j(t_0)_2 - \phi_A(t_0)_2 + N_{A2}^j]$$

Where:

$\Delta PD_{L_1}$  and  $\Delta PD_{L_2}$  are the observed pseudo ranges minus those calculated as a function of the approximated parameters, for  $L_1$  and  $L_2$ , respectively;

$\Delta X_A$ ,  $\Delta Y_A$  and  $\Delta Z_A$  are the corrections to the approximated parameters  $X^0$ ,  $Y^0$  and  $Z^0$  in order to obtain  $X$ ,  $Y$  and  $Z$ ;

$\Delta \phi_{A1}^j$  and  $\Delta \phi_{A2}^j$  are the observed minus the calculated carrier phases, as a function of the approximated parameters for  $L_1$  and  $L_2$ , respectively;

$\lambda_1$  and  $\lambda_2$  are the wavelengths of the  $L_1$  and  $L_2$  carriers, respectively;

$I_A^j$  and  $\bar{I}_A^j$  refer to the ionospheric refraction in the  $L_1$  and  $L_2$  carriers, for the satellite  $j$ ;

$\phi^j(t_0)_1$  and  $\phi^j(t_0)_2$  are the  $L_1$  and  $L_2$  carrier phases, generated in the satellite  $j$ , for a reference epoch  $t_0$ ;

$\phi_A(t_0)_1$  and  $\phi_A(t_0)_2$  are the  $L_1$  and  $L_2$  carrier phases, generated in the receptor  $A$ , for a reference epoch  $t_0$ ;

$N_{A1}^j$  and  $N_{A2}^j$  represent the ambiguities in the carriers  $L_1$  and  $L_2$ , respectively;

$a_A^j$ ,  $b_A^j$  and  $c_A^j$ , refer to the partial differential of the geometric range with relation to the approximated parameters;

$E(.)$  is the expectation operator.

This procedure involves four observables for each of the visible satellites in each epoch. The two pseudo range and carrier phase observables can be linearly combined, thus reducing the effects of the ionospheric refraction. The use of a tropospheric model, together with parameterisation techniques, can reduce the tropospheric refraction effects. The IGS ephemerides supply satellite coordinates and clock errors, with accuracy in the order of 5 cm and 0.3 ns, respectively, and are essential in PPP.

With this procedure, most of the GPS observation errors are reduced. However, variations due to geophysical phenomena should be removed using appropriate models. These corrections include (McCarthy, 1996):

polar motion;

atmospheric load;

Earth body tides and ocean tide loading.

According to Zumerge et al. (1997), with PPP it is possible to obtain precision of a few millimeters and a few centimeters in the horizontal and vertical components, respectively. Such levels of accuracy can be obtained for static point positioning, using a period of 24 hours of data (Monico and Perez, 2001; Monico, 2000a).

Once the coordinates for all stations are daily estimated using PPP, a solution for a specific epoch  $t$  can be

obtained. As there is no correlation between the coordinates of different stations, such a solution may be obtained independently for each station. Considering a station  $i$ , with solutions at epochs  $t_1, t_2, \dots, t_n$ , and assuming a constant velocity for the considered period, the final solution is given by:

$$\begin{bmatrix} X_t \\ V_t \end{bmatrix} = \begin{bmatrix} \sum_{i=1}^n P_i & \sum_{i=1}^n (t-t_i)P_i \\ \sum_{i=1}^n (t-t_i)P_i & \sum_{i=1}^n (t-t_i)^2 P_i \end{bmatrix}^{-1} \begin{bmatrix} \sum_{i=1}^n P_i X_i \\ \sum_{i=1}^n (t-t_i)P_i X_i \end{bmatrix} \quad (3)$$

Where  $P_i$  is the weight matrix obtained from the inverse of the covariance matrix  $\sum X_i$ ,  $X_i = [x, y, z]^T$  is the coordinate vector estimated from the several GPS solutions, and  $V_i = [v_x, v_y, v_z]^T$  is the estimated velocity vector.

#### 4 Estimation of the Plate Rotation Vector

Using the velocities  $v_x$ ,  $v_y$  and  $v_z$  and the respective coordinates of the stations estimated by GPS, it is possible to estimate the rotation Euler vector ( $\Omega_x$ ,  $\Omega_y$  and  $\Omega_z$ ) in a Least Square adjustment. Using the very well known Euler theorem, eq. (4) gives the linearized observation equation for one station (Drewes, 1993):

$$\begin{bmatrix} v_x \\ v_y \\ v_z \end{bmatrix} = \begin{bmatrix} 0 & -\Omega_z & \Omega_y \\ \Omega_z & 0 & -\Omega_x \\ -\Omega_y & \Omega_x & 0 \end{bmatrix} \begin{bmatrix} x \\ y \\ z \end{bmatrix} = \omega \times X \quad (4)$$

It is also possible to write an observation equation similar to eq. (4) based on the spherical coordinates.

Tab. 1 RBMC and IGS stations.

Station	Identification	Country	Tectonic Plate	Network
Bom Jesus	BOMJ	Brazil	SOAM	RBMC
Brasília	BRAZ	Brazil	SOAM	RBMC and IGS
Cuiabá	CUIB	Brazil	SOAM	RBMC
Fortaleza	FORT	Brazil	SOAM	RBMC and IGS
Imperatriz	IMPZ	Brazil	SOAM	RBMC
Manaus	MANA	Brazil	SOAM	RBMC
Curitiba	PARA	Brazil	SOAM	RBMC
Porto Alegre	POAL	Brazil	SOAM	RBMC
Recife	RECF	Brazil	SOAM	RBMC
Salvador	SALV	Brazil	SOAM	RBMC
Pres. Prudente	UEPP	Brazil	SOAM	RBMC
Viçosa	VICO	Brazil	SOAM	RBMC
Ascension	ASC1	United Kingdom	SOAM	IGS
Easter Island	EISL	Chile	NAZC	IGS
Fairbanks	FAIR	USA	NOAM	IGS
Goldstone	GOLD	USA	NOAM	IGS
La Plata	LPGS	Argentina	SOAM	IGS
Pinyon Flats	PIN1	USA	PCFC	IGS
Santiago	SANT	Chile	SOAM	IGS
Sutherland	SUTH	South Africa	AFRC	IGS

## 5 Methodology: Software, Data Set and Strategy Adopted

### 5.1 Software and Data Set

The software used for the processing of the GPS data is GIPSY OASIS II (GPS Inferred Positioning SYstem – Orbit Analysis and Simulation Software), or simply, GOA II (Gregorius, 1996). GOA II is capable of PPP processing as well as other processing techniques.

This research used data from a total of 20 stations. Of these, 12 belong to RBMC, 2 of which also belong to IGS (Fortaleza and Brasília). The other 8 are IGS stations. These stations are located on the following tectonic plates: South American (SOAM), African (AFRC), Nazca (NAZC), North American (NOAM) and Pacific (PCFC). Stations located on plate boundaries were also included, to identify the effect of this location on station movements. Table 1 provides information on the 20 stations used in the processing, and Figure 2 shows their location.

Data was collected over a period of almost 3 years. The initial observations were made on June 28, 1998, and the

final observation on April 1, 2001. The data is divided in to 6 sub-periods of 15 days each, such that all different climatic seasons of the year were considered.

The reference epoch adopted in the processing was March 19, 2000 ( $t = 2000.2$ ), which refers to the average epoch of the period. Therefore, the solution will be referenced to ITRF 97, epoch 2000.2.

### 5.2 Strategy Adopted in the Processing of GPS Data

The processing was carried out using the GOA II software for PPP, and the IGS ephemerides produced by JPL (Jet Propulsion Laboratory). These ephemerides are referenced to ITRF 97, and the epoch refers to each day of observation. The basic observable was ionosphere free, with 30 seconds recording interval and elevation mask of  $15^\circ$ . The ambiguities were not solved as integers. The standard algorithm to correct for effects caused by earth body tides, ocean tide loading and polar motion were used, and can be found in the IERS Standards (McCarthy, 1996).

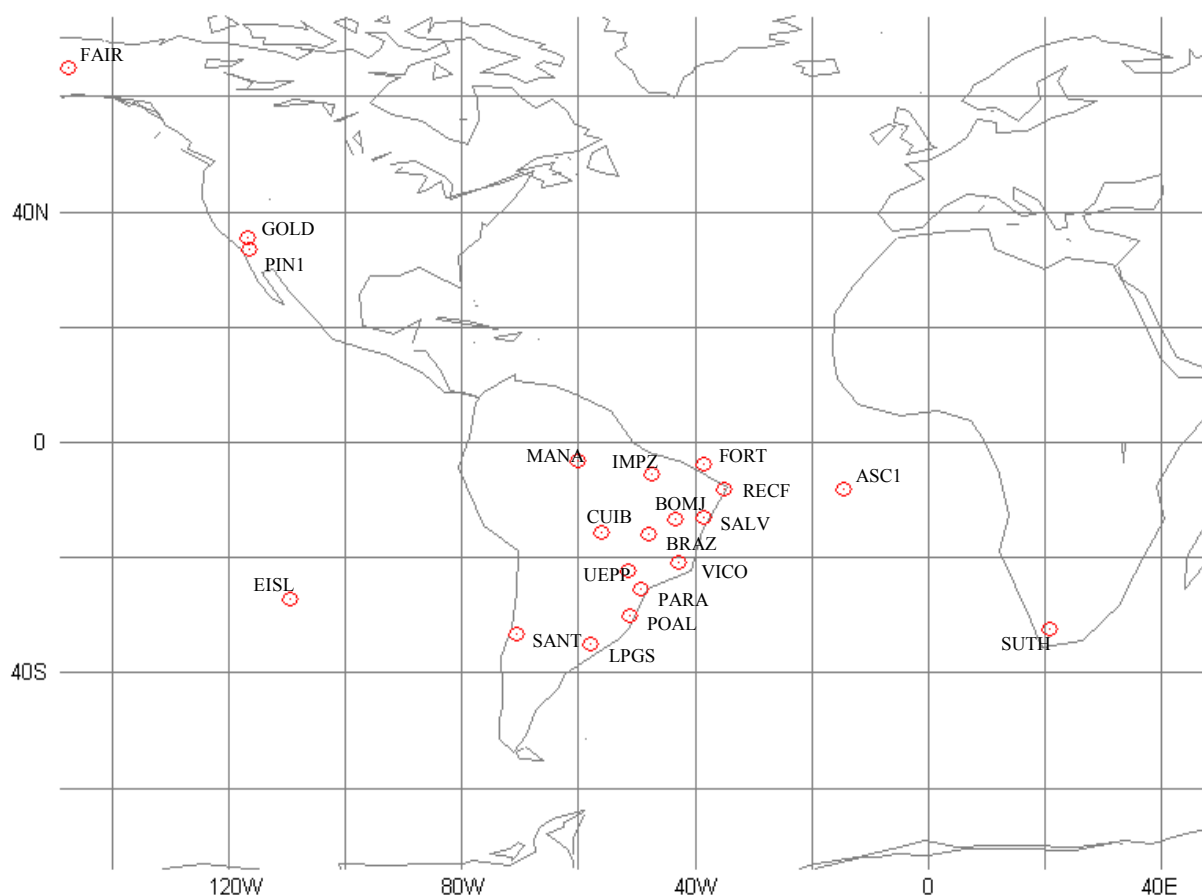


Fig. 2 Location of the RBMC and IGS stations.

### 6 Analyses of the Results

The precision and accuracy of the coordinates and velocity components of the stations, in terms of a local geodetic coordinate system ( $N, E, u$ ), are analysed.

#### 6.1 Precision

The precision analysis is based on two criteria:

- the formal standard deviations of the coordinates and velocity components;
- the repeatabilities of the estimated coordinates.

The formal standard deviation of the parameters is obtained from the MVC (Variance and Covariance Matrix) of the parameters. It is an expression that usually provides very optimistic values for the quality of the parameters (Monico and Perez, 2001; Monico, 2000a).

The daily repeatability (REP) provides a more realistic measure of precision for station coordinates. It is the weighted quadratic averaged error, which is given by the expression (Blewitt, 1989):

$$REP = \left( \frac{\frac{n}{n-1} \sum_{i=1}^n \frac{(R_i - \bar{R}_m)^2}{\sigma_i^2}}{\sum_{i=1}^n \frac{1}{\sigma_i^2}} \right)^{\frac{1}{2}} \quad (5)$$

where  $n$  is the number of occupation days,  $R_i$  is the estimated coordinate and  $\sigma_i$  is the formal error (standard deviation) of the coordinates for day “ $i$ ”, and  $\bar{R}_m$  is the weighted mean of the coordinates of the station.

Figures 3 and 4 illustrate the precision of the station coordinate components ( $N, E, u$ ), in terms of the standard deviation and repeatability, respectively. The figures illustrate that for most of the stations, the repeatabilities of the height component ( $u$ ) (Figure 4) is 2 or 3 times worse than the respective standard deviation (Figure 3). Other stations, such as PIN1, show a greater difference with height repeatabilities of one order of magnitude larger than the standard deviation. The repeatability of component  $E$  is 3 to 4 times worse than the standard deviation for most of the stations. In some cases the values are 10 to 20 times worse, as is the case for EISL. This could be due the number of cycle slips in the EISL observation data. For component  $N$ , most of the station repeatability values are approximately 10 times worse than their respective standard deviations. As expected, the standard deviation and repeatability values are worse for the height component. The better quality of  $N$  components in relation to the  $E$  one is due to the fact that the ambiguities were not solved.

Figure 5 shows the formal precision of the velocities in a local geodetic coordinate system, in terms of horizontal ( $V_{Horiz}$  - resultant of  $V_N$  and  $V_E$ ) and height ( $V_u$ ) components.

The formal precision of both components ( $V_{Horiz}$  and  $V_u$ ) is less than 1.3 mm/year, for all stations. Like the coordinates, it is expected that these values are very optimistic. On average, the horizontal and vertical precision of the velocity components are approximately the same. From the results presented here, on average it reaches 0.6mm/year (see Figure 5).

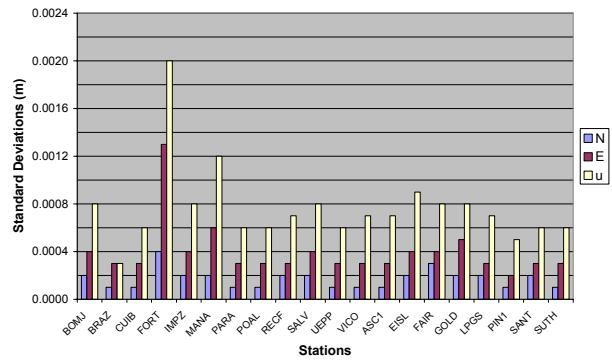


Fig. 3 Standard deviations of the coordinate components (N, E, u).

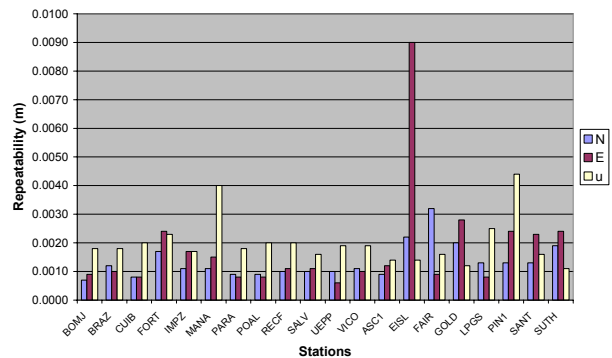


Fig. 4 Repeatability of the coordinate components (N, E, u).

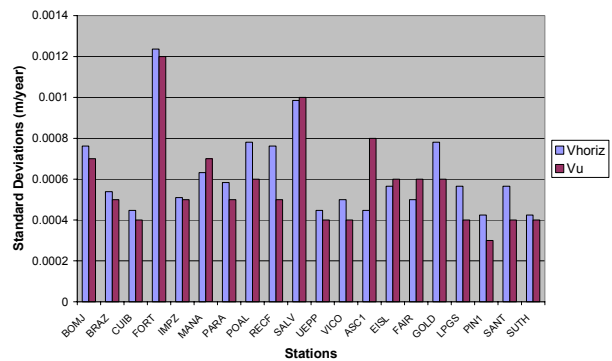


Fig. 5 Standard deviations of the velocities ( $V_{Horiz}, V_u$ ).

### 6.2 Accuracy

A comparison of the results obtained in this work with those supplied by other sources, such as ITRF and geophysical models, allow an evaluation of the accuracy of the obtained solutions. Statistical quantities required include: the mean error, the standard deviation ( $\sigma$ ), and the mean square error (MSE).

These statistical quantities, allow a comparison with the accuracy of the coordinates and velocities, from ITRF solutions, and NNR-NUVEL 1A and APKIM 2000 models.

Figure 6 shows the difference between the final coordinates of this solution and those supplied in the ITRF 2000. In Figure 7 the difference between the velocities of the final solution and those supplied in the ITRF 2000 are illustrated. The ITRF 2000 coordinates and velocities were transformed to ITRF 97 (epoch 2000.2). Hereafter, this solution will be identified by ITRF2000/97.

Figures 6 and 7 show that component  $u$  presents the largest differences. From Figure 6 it can be seen that the difference in the MSE of  $u$  is around 1cm, while for the  $N$  and  $E$  components the difference is 2.1 mm and 4.4 mm, respectively.

In Figure 7 the difference in MSE of  $u$  is about 1.3 cm/year, while the difference in  $N$  and  $E$  is a maximum of 6 mm/year. The maximum discrepancies between the final velocity solution and ITRF 2000/97 are 3.0 and 2.0 cm/year for the height components of stations MANA and IMPZ, respectively. These two stations gave the worst results for the Brazilian ITRF 2000 stations. Their ITRF 2000 height precisions are 19.8 and 18.6 mm/year respectively, which may explain the large difference in the velocity comparisons (see <http://lareg.ensg.ign.fr/ITRF>) (access date: October 20, 2003)). By omitting these 2 stations from the analysis, the average MSE of the height component reduces to 7mm/year, which approximately represents the uncertainty of the ITRF2000 for most of the Brazilian stations. Therefore, the differences mainly represent the uncertainty of the ITRF2000 solution.

The difference between the velocities of the final solution and those of the geophysical model NNR-NUVEL 1A and APKIM 2000 are shown in Figures 8 and 9.

Figures 8 and 9 show that the largest differences occur at stations PIN1 and SANT. This may be due to their location on plate boundaries, where deformations are less accurately modeled.

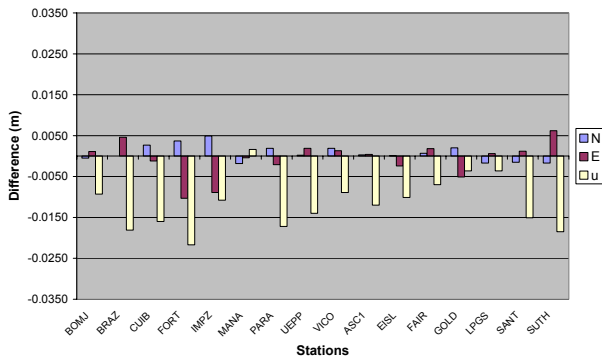


Fig. 6 Difference between the coordinates of the final solution and the coordinates of ITRF 2000/97.

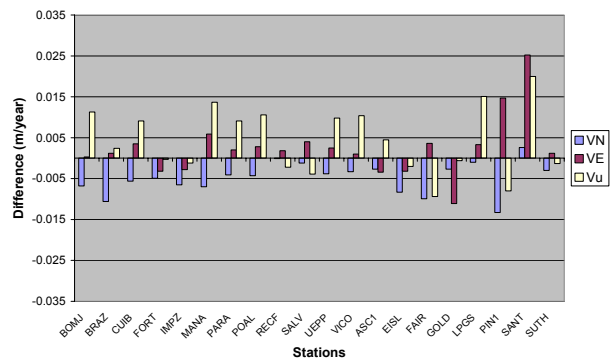


Fig. 8 Difference between the velocities of the final solution and the velocities of NNR-NUVEL 1A model.

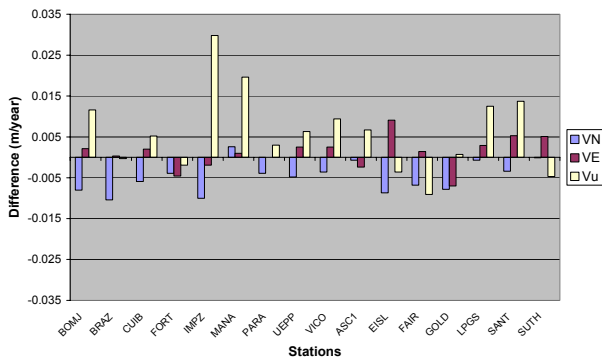


Fig. 7 Difference between the velocities of the final solution and the velocities of ITRF 2000/97.

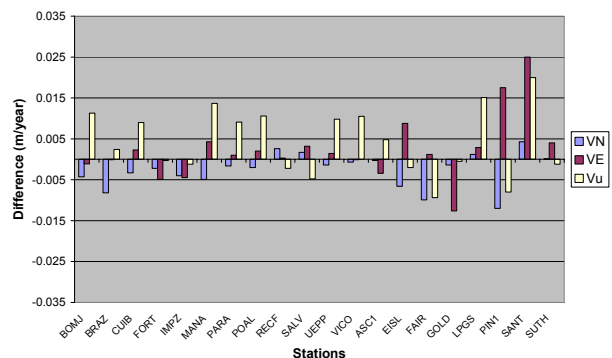


Fig. 9 Difference between the velocities of the final solution and the velocities of APKIM 2000 model.

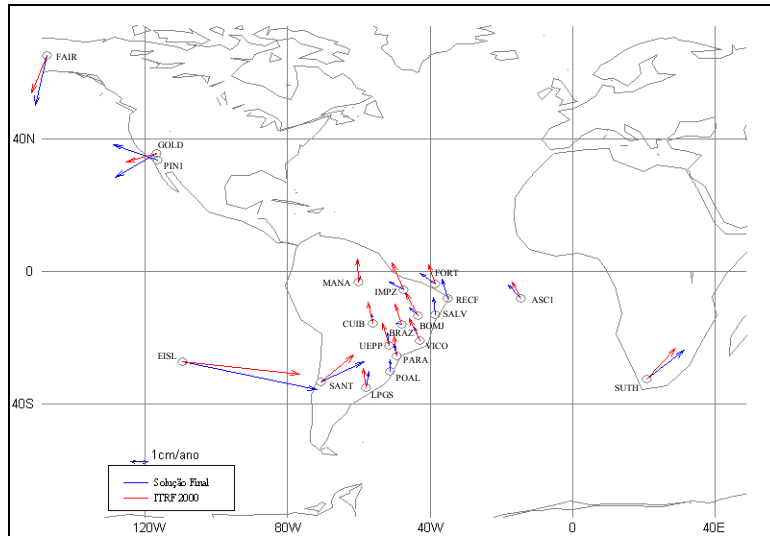


Fig. 10 Velocity Field of the Final Solution and ITRF 2000/97.

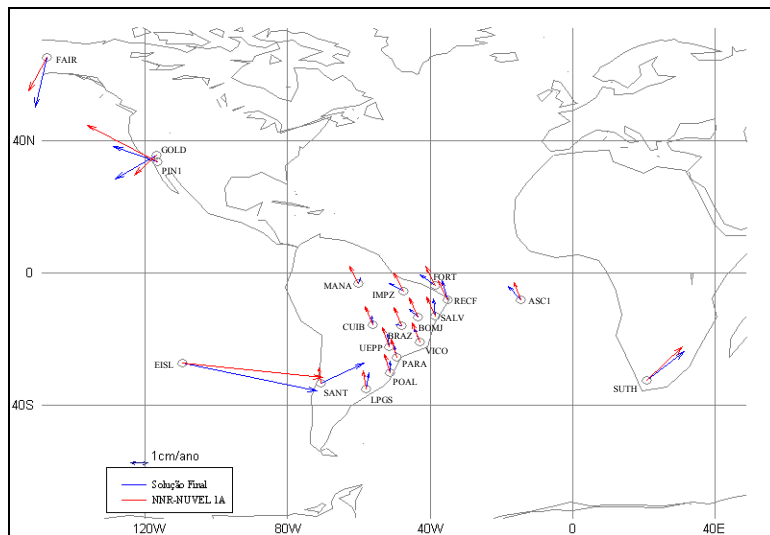


Fig. 11 Velocity Field of the Final Solution and NNR-NUVEL 1A model.

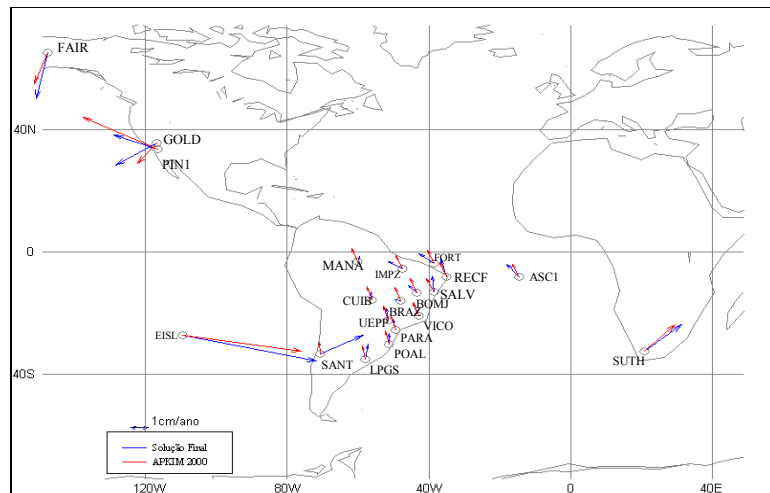


Fig. 12 Velocity of the Final Solution and APKIM 2000 model.

In can be seen that the velocity difference between the geophysical models and the final solution (Figures 11 and 12) is greater for stations PIN1 and SANT, than when compared with the ITRF2000/97 solution (Figure 10). Such results represent the effectiveness of using GPS PPP as a tool for geodynamics in the estimation of station velocity.

Figures 10 to 12 illustrate the horizontal velocity field in the local geodetic system components (N, E) obtained from the final PPP solution, compared with the ITRF2000/97 solution, NNR-NUVEL 1A, and APKIM 2000.

Stations located in the Brazilian territory, a very stable portion of SOAM plate, show good agreement between each of the solutions in Figures 10, 11 and 12. However, the final solution of stations SANT, PIN1 and GOLD are notably different to the NNR-NUVEL 1A and APKIM 2000 modeled solutions. Figure 13, adapted from Turcotte and Schubert (2001), shows the locations of stations SANT, PIN1 and GOLD.

Stations SANT, PIN1 and GOLD are located alongside plate boundaries. Stations PIN1 and GOLD are located on opposite sides of the San Andreas transform fault, in California, hence the different directions of movement at these stations. SANT is located on a subduction zone. Complex and relatively significant deformations occur on subduction plate boundaries, which may not be well represented by a geophysical model. More detailed investigations related to the deformation in the region of this station can be found in Kendrick et al. (2001) and Brooks et al. (2003).

It is worth noting that the largest movement were observed on the Easter Island station (EISL), located on

the Nazca plate. Similar results were obtained also for the ITRF solutions and the NNR-NUVEL 1A and APKIM 2000 models.

### 7 SOAM PLATE Rotation Vector Estimation

Using the velocities  $v_x$ ,  $v_y$  and  $v_z$ , with the respective coordinates of the stations, the rotation vectors ( $\Omega_x$ ,  $\Omega_y$  and  $\Omega_z$ ) of the SOAM plate have been estimated using Least Squares adjustment. The full covariance matrix was considered and the observation equation is given in equation (4).

Table 2 presents the rotation vectors for the ITRF2000 results and the results of this research, identified as partial solutions. The vectors are estimated from stations LPGS (La Plata), FORT and ASC1 (Ascension), which are the stations used for computing the ITRF 2000 SOAM rotation vectors. Each rotation parameter is given in radians per million of years (rad/My), and the module of the Euler vector ( $\varpi$ ) is in degrees per million of years ( $^{\circ}/My$ ).

Tab 2 – Rotation vectors for the SOAM Plate

MODEL	$\Omega_x$ (rad/My)	$\Omega_y$ (rad/My)	$\Omega_z$ (rad/My)	$\varpi$ ( $^{\circ}/My$ )
Partial Solution	-0,00110	-0,00192	-0,00085	0.1359
ITRF 2000	-0.00105	-0.00122	-0.00022	0.1130

It can be seen from Table 2 that the discrepancies between solutions reach a maximum of 2.4 mm/year ( $1''/My$  in  $\varpi \sim 0.03$  mm/year at equator). The precision of

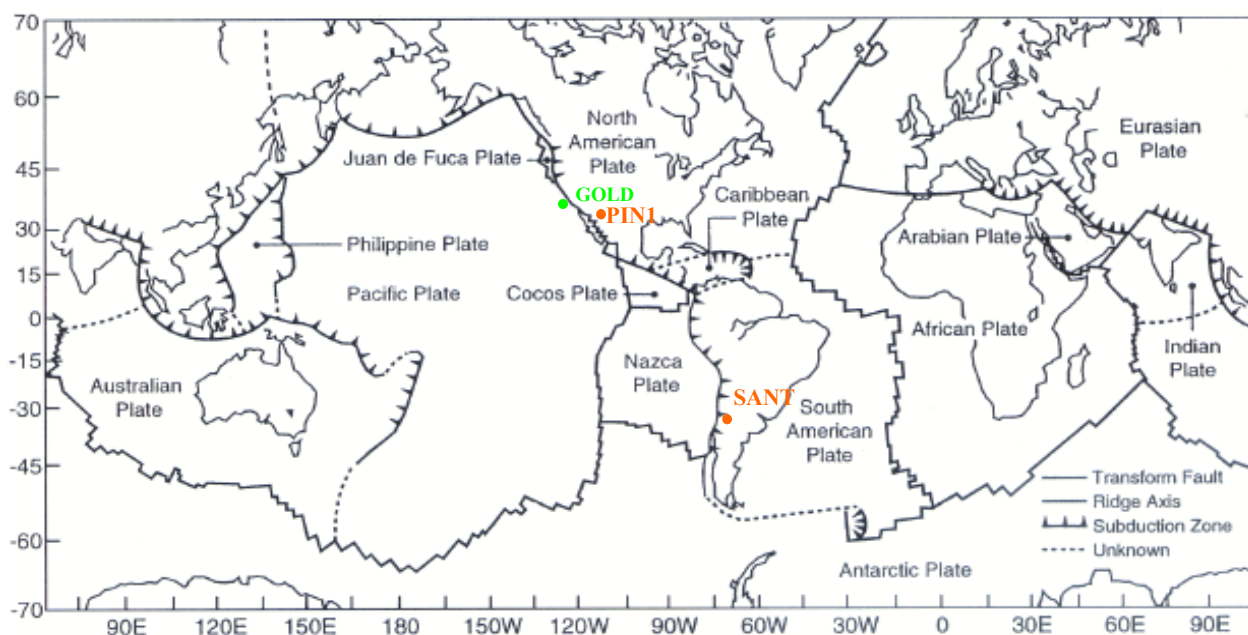


Fig. 13 Location of the stations with the largest differences in relation to the geophysical models.



the ITRF2000 solution for the velocity of the stations involved in this analysis is of the order of 1.7 mm/year (<http://lareg.ensg.ign.fr/ITRF>), whilst the precision of the PPP solutions is generally less than 0.8mm/year (Figure 8).

In Table 3 additional stations observed in this research are incorporated into the rotation vector estimation. The 14 stations used include: BOMJ, BRAZ, CUIB, FORT, IMPZ, MANA, PARA, POAL, RECF, SALV, UEPP, VICO, ASC1 and LPGS (see Table 1). The APKIM2000, NUVEL 1-A and ITRF2000 results are also presented.

Tab 3 – Final Rotation vectors for the SOAM Plate and of other sources

MODEL	$\Omega_X$ (rad/My)	$\Omega_Y$ (rad/My)	$\Omega_Z$ (rad/My)	$\varpi$ (°/My)
Final Solution	-0.00090	-0.00186	-0.00073	0.1257
ITRF 2000	-0.00105	-0.00122	-0.00022	0.1130
NNR-NUVEL 1A	-0.00104	-0.00152	-0.00087	0.1164
APKIM2000	-0.00095	-0.00116	-0.00060	0.0925

The results presented in Table 3 show a slightly better agreement between the PPP and ITRF2000 solutions, reaching a maximum difference of 1.5 mm/year. This value is in agreement with the ITRF2000 uncertainty for the stations involved in this estimation. When compared with NNR-NUVEL 1-A, the maximum difference reduces to 1.2 mm/year. The poorest results are from the APKIM model. This was unexpected since it is based on GPS, SLR and VLBI measurements. The discrepancy can reach 3.7 mm/year. However, the more recent APKIM 2002 version brings the result more in line with the other models (Drewes, 2003).

## 8 Comments and Conclusions

A very brief introduction to plate tectonics was presented together with the application of PPP for estimating the velocity field of stations located on the SOAM Plate. Stations on other plates were also included in order to infer our solution with those provided from other sources.

The velocities obtained from ITRF2000 solutions and those derived from the NNR-NUVEL 1A and APKIM 2000 models were compared with the final PPP solution. The comparison with the ITRF 2000 solution showed a general agreement, when stations MANA and IMPZ were omitted. The PPP solutions were in the range of the ITRF2000 precision of the Brazilian stations. The comparison with models NNR-NUVEL 1A and APKIM 2000 showed that the largest discrepancies are for stations located close to plate boundaries. It is an expected result, since these models do not take into account the deformation that occurs in such regions. This

highlights the potential of GPS for velocity determination at plate boundaries.

The comparison between the estimated rotation vector from the PPP solution with the rotation vectors determined from other sources provided very good results. The rotation vector estimates derived from the PPP solutions could potentially provide a new model for South American plate motion at stations without an estimated velocity vector. The new model incorporates a greater number of stations than the ITRF 2000 rotation vector estimation, and is not subject to the discrepancies due to uncertainty in the geophysical models.

Finally, it can be concluded that PPP is a positioning method that can feasibly be applied to applications requiring a high level of precision, such as the estimation of station coordinates and velocity vectors, as well as the plate rotation vector.

## Acknowledgments

FAPESP provided the financial support (process number 00/08521-0). IBGE and JPL provided the GPS data and ephemerides, respectively. We thank the two anonymous reviewers for suggesting improvements to our original manuscript.

## References

- Altamimi, Z., P. Sillard and C. Boucher (2002) *ITRF 2000: A New Release of the International Terrestrial Reference Frame for Earth Science Applications*, Report of the Institut Géographique National, Paris, France.
- Blewitt, G. (1989) *Carrier Phase Ambiguity Resolution for the Global Positioning System Applied to Geodetic Baselines up to 2000 km*, Journal of Geophysical Research, Vol. 94, No. B8, 10.187-10.203.
- Brooks, B. A., M. Bevis, R. K. Smalley, M. René; E. Lauria; R. Maturana and M. Araujo (2003) *Crustal Deformation in the Southern Andes (260–360): Do the Andes behave like a microplate*, Geochemistry, Geophysics, Geosystems, Vol. 4, No. 10.
- Condie, K. C. (1989) *Plate Tectonics & Crustal Evolution*, Third Edition, New Mexico Institute of Mining and Technology, Socorro, New Mexico, 476 p.
- Costa, S. M. A. (1999) *Integração da Rede Geodésica Brasileira aos Sistemas de Referência Terrestres*, Tese de Doutorado, UFPR, Curitiba, 156 p.
- Drewes, H. (2003) *Personal Communication during the XXI Brazilian Congress of Cartography*.
- Drewes, H. (1993) *Global and Regional Deformation Models of the Earth's Surface*, In Sevilla M.J., H. Henneberg, R. Viera (Eds.), Proceedings of the International Conference

- on Cartography and Geodesy, Maracaibo (Venezuela), Instituto de Astronomia y Geodesia, Madrid, 288-298.
- Drewes, H. (1996) *Sistema de Referência Cinemático Global Incluindo um Modelo do Movimento Actual de las Placas Tectónicas*, IV Congresso Internacional de Ciencias de la Tierra, p. 230, Santiago.
- Fortes, L. P. S. (1997) *Operacionalização da Rede Brasileira de Monitoramento Contínuo do Sistema GPS (RBMC)*, Dissertação de Mestrado, IME, 1997, 152 p.
- Gregorius, T. (1996) *GIPSY-OASIS II: How it works*, Department of Geomatics, University of Newcastle upon Tyne, 152 p.
- Hoffmann-Wellenhof B., H. Lichtenegger and J. Collins (2001) *Global Positioning System Theory and Practice*, Wien: Springer-Verlag, 5 ed. (revised), 382 p.
- Kendrick, E. M. Bevis, R. Smalley and B. Brooks (2001) *An integrated velocity field estimation for the Central Andes*, Geochemistry, Geophysics, Geosystems, Vol. 2, Paper number 2001GC000191.
- Leick, A. (1995) *GPS Satellite Surveying*, New York: John Wiley & Sons, 560 p.
- McCarthy D. D. (1996) *IERS Conventions: IERS Technical Note 2*, Central Bureau of IERS – Observatoire de Paris, 95 p.
- Monica, J. F. G. (2000) *Posicionamento pelo NAVSTAR-GPS: Descrição, Fundamentos e Aplicações*, Editora UNESP, São Paulo, 287 p.
- Monico, J. F. G. (2000a) *Posicionamento por Ponto de Alta Precisão: Uma Ferramenta para a Geodinâmica*, Revista Brasileira de Geofísica. Rio de Janeiro, RJ, Vol. 18, No. 1, p. 1-10.
- Monico, J. F. G. and J. A. S. Perez (2001) *Integration of a Regional GPS Network within ITRF using Precise Point Positioning*, In Adam, J., K.P. Schwarz (Org.) Vistas for Geodesy in the new millennium: IAG Scientific Assembly, Berlin, Vol. 125, p. 66-71.
- Parkinson, B. W. (1996) *Introduction and Heritage of NAVSTAR, the Global Positioning System*, In Parkinson, B. W. and J. J. Spilker Jr. Global Positioning System: Theory and Applications, Cambridge: American Institute of Aeronautics and Astronautics, Vol.1, 793 p.
- Perez, J. A. S. (2002) *Campo de Velocidade para as Estações da RBMC e do IGS localizadas na Placa Sul-Americana: Estimativa a partir do Processamento de Dados GPS*, Dissertação de Mestrado, FCT-UNESP, Presidente Prudente, 166 p.
- Press, F. and R. Siever (1986) *Earth*, Fourth Edition, W. H. Freeman and Company, New York, 656 p.
- Sá, N. C. (1999) *GPS: Fundamentos e Aplicações*, Departamento de Geofísica, IAG-USP, 87 p.
- Seeber, G. (2003) *Satellite Geodesy: Foundations, Methods and Applications*, Walter de Gruyter, N. York, 2<sup>nd</sup> Edition, 589 p.
- Turcotte, D. L. and G. Schubert (2001) *Geodynamics*, Second Edition, Cambridge University Press, United Kingdom, 456 p.
- Van Dam, T. M. and J. M. Wahr (1987) *Displacements of the Earth's Surface Due to Atmospheric Loading: Effects on Gravity and Baseline Measurements*, Journal of Geophysical Research, Vol. 92, No. B2, p. 1281-6.